



SYNTHESIS OF CORE-SHELL $\text{Fe}_3\text{O}_4/\text{C18}/\text{SiO}_2/[\text{3 (2-Aminoethyl amino) propyl}]$ TRIMETHOXY SILANE AND THE STUDY OF THE ADSORPTION KINETICS MODEL OF Cu^{2+} AND Cr^{6+} IONS

Mighfar Syukur* and Ahmad Fuad Masduqi

¹Departmen Pharmacy, Semarang Pharmaceutical College,
Jl. Letjend Sarwo Edhie Wibowo KM 1, Plamongsari, Semarang, 50192, Central Java, Indonesia

* Untuk korespondensi: e-mail: syukurads@yahoo.co.id

Received: December 10, 2019

Accepted: May 15, 2020

Online Published: Aug 26, 2020

DOI : 10.20961/jkpk.v5i2.37820

ABSTRACT

Synthesis of Core-Shell $\text{Fe}_3\text{O}_4/\text{C18}/\text{SiO}_2/[\text{3 (2-Aminoethyl amino) propyl}]$ Trimethoxy silane has been conducted to study its adsorption kinetics of Cu^{2+} and Cr^{6+} ions. Fe_3O_4 synthesis was carried out to form cores that have magnetic properties. The aim of the coating $\text{C18}/\text{SiO}_2/[\text{3(2-Aminoethylamino) propyl}]$ trimethoxy silane was to protect these cores from physical degradation due to acids and bases, as well as the application of synthetic materials. The sono-coprecipitation method showed good results under N_2 gas flow with the results of black crystals. The success of SiO_2 and $[\text{3(2-Aminoethylamino) propyl}]$ coatings the transformation of the color showed Trimethoxy silane into brown and weight gain of the synthesis result. Analysis of XRD data showed that little Fe_2O_3 impurities were clarified by FTIR data showing the presence of amine groups from the starting material. The SEM-EDX and TEM showed a spherical shape with a core-shell system. The adsorption kinetics model was studied using two kinetics models for Cu^{2+} and Cr^{6+} ions. The results were demonstrated by the suitability of Cu adsorption to the pseudo order 1, with an adsorption rate of 0.0333 min^{-1} , whereas for Cr corresponded to pseudo order 2 with an adsorption rate of $0.00536 \text{ gM}^{-1}\text{min}^{-1}$.

Keywords: Coating, kinetics, core-shell, Synthesis, Fe_3O_4 / C18

INTRODUCTION

Magnetic nanoparticles (MNPs) are interesting materials to be researched and developed because they are based on their size and nature. They have very broad applications in terms of data storage, biochemistry, biosensors, magnetic resonance images (MRI), and drug delivery systems [1]. The effort to increase the size and shape of magnetic nanoparticles or monodisperse system with nanometer dimensions is one of the important keys because the magnetic

strength properties depend on their sizes and dimensions[2], [3].

Synthesis of magnetite nanoparticles can be done by various methods such as coprecipitation, thermal decomposition, hydrothermal, microemulsion, and sonochemical [4], which can produce a variety of nanoparticle size. Despite the fact that there are many different types of nanoparticles, MNPs are particles that are often used in making the core, because the coating material can be modified with organic or inorganic material with the addition of various lots of functions

[5], [6]. For example, magnetic nanoparticles are used as a detector of the immune system bypassing blood circulation. This material is stable for a long time in the circulatory system [7].

The coating material on the surface of magnetic nanoparticles will increase chemical stability. This stability protects the magnetic core from degradation at high temperatures, oxidation by oxygen in the air, or erosion by acids and bases [8], [9]. Silica is one of the compounds used in coating the magnetite core, so it has some advantages such as: not only protecting from physical stability but also preventing of agglomeration of the particles, controlling the thickness of the coating, and ease of surface modification with other organic compounds [10]. While the addition of organic functional groups on MNPs/Silica (SiO_2), has a significant influence on biological ability and biodegradability. Addition of groups that can be done between aldehydes, hydroxyl groups, carboxyl groups, and amino groups [11].

Modified Synthesis of Fe_3O_4 cellulose modified chitosan and polyacrylamide was used in decreased levels of Cu (II) in waste water [12], [13]. Decreasing of Cr (IV) level was also done by modifying the surface of magnetite or silica with amino groups [14], [15]. Although various group modifications have been made, the application into waste was still limited to one metal with the same charge. In this research, the synthesis of Fe_3O_4 nanoparticles was carried out with the addition of oleic acid (C18) with the combined sono-coprecipitation method at room temperature, with precursors of FeCl_3 and FeSO_4 . As prevention of

agglomeration, a SiO_2 coating was carried out with modification of diamino group that would be bound to the surface so that it has a function in the adsorption of Cu^{2+} and Cr^{6+} ions. The adsorption kinetics was studied by using two-equation models that got the results of the rates of adsorption reaction. The data rate of the reaction was useful to study the possible mechanism of adsorption reactions that occur, and this data can be used to measure the performance of the adsorbent in the adsorption process.

METHODS

1. Materials

$\text{FeCl}_3 \cdot 6\text{H}_2\text{O}$ (Merck), FeSO_4 (Pudak), NH_3 25% (Merck), oleic acid/OA (technical), Ethanol 98% (Merck). The ingredients for coating Fe_3O_4 include Na_2SiO_3 (technical), [3-(2-Aminoethyl amino) propyl] Trimethoxy silane (Aldrich), methanol 97% (Merck), HCl 37% (Merck) to study the reaction kinetics used: $\text{CuSO}_4 \cdot 5\text{H}_2\text{O}$ (Merck), K_2CrO_4 (Pudak), KCl (Merck), potassium hydrogen phthalate (Merck), and KH_2PO_4 (Merck), KH Phthalate (Merck), NaOH (Merck) and demineralized water (Brataco).

2. Synthesis of Fe_3O_4 coated C18

Synthesis of Fe_3O_4 coated with Oleic Acid using the sono-coprecipitation method was carried out by weighing 0.02 mol of $\text{FeCl}_3 \cdot 6\text{H}_2\text{O}$, and 0.0138 mol of $\text{FeSO}_4 \cdot 7\text{H}_2\text{O}$ dissolved in 60 mL demineralized water under N_2 gas flow. 25% NH_3 3.5 mL was added to the system quickly, of 1000 mg of oleic acid solution that was put into solution and cultivated for 1 hour. The solution was

then rinsed with distilled water and ethanol, then dried at > 80 °C

3. Synthesis of Fe₃O₄/C18/SiO₂/[3(2-Aminoethyl amino) propyl] Trimethoxy silane

0.5 g Fe₃O₄/C18 is washed with 5 mL dilute HCl in 10 mL methanol. With the principle of the sol-gel method, add [3(2-Aminoethyl amino) propyl] Trimethoxy silane and Na₂SiO₃ were the stirring processes for 3 hours.

The solution was treated for 24 hours and washed again with aqua bides. The residue was separated by an external magnet, dried at temperatures > 80 °C.

4. Characteristic of Fe₃O₄/C18/SiO₂/[3(2-Aminoethyl amino) propyl] Trimethoxy silane

Testing the crystalline diffraction patterns of Fe₃O₄ and Fe₃O₄/C18/SiO₂/[3(2-Aminoethyl amino) propyl] Trimethoxy silane to see the successful synthesis was carried out with X-Ray Diffraction (XRD). Particle composition can be analyzed by using Scanning Electron Microscopy-Energy Dispersive X-Ray (SEM-EDX), while the particle size can be predicted through Transmission Electron Microscopy (TEM). Adsorption testing was performed with Atomic Absorption Spectroscopy (AAS).

5. Adsorption Kinetics of Cu²⁺ and Cr⁶⁺

Adsorption kinetics model in this study was conducted by optimizing the pH of the two solutions of Cu and Cr are at pH 1,2,3,4,5,6 and 7 at a concentration of 20 ppm. In the next stage, the adsorption process was carried out with different contact times at 15, 30, 45, 60, and 75 minutes for the study of adsorption kinetics at a concentration of 30 ppm. Kinetic modeling is done by Lagergren first-order kinetics model [16], and McKay & Ho kinetics model [17]. The equation for Frist-Order Lagergreen is:

$$\text{Log}(q_e - qt) \log q_e - \left(\frac{k_1}{2,303}\right)t \dots\dots\dots(1)$$

The equation for the Pseudo Second-Order McKay & Ho kinetics is formulated as follows:

$$\frac{t}{qt} = \frac{1}{kq_e^2} + \frac{1}{q_e}t \dots\dots\dots(2)$$

Where *k₁* is the pseudo-order adsorption rate constant, *k* is the pseudo-order second rate constant, *q_e* is the number of ions adsorbed at equilibrium, and *qt* is the number of ions adsorbed at Table 1.

Table 1. Synthesis of Fe₃O₄/C18 and Fe₃O₄/C18/SiO₂/[3(2-Aminoethyl amino) propyl] Trimethox silane

Synthesis Fe ₃ O ₄ /C18	Weight (g)	Synthesis of Fe ₃ O ₄ /C18/SiO ₂ /[3(2-Aminoethyl amino) propyl] Trimethoxy silane (g)	Weight (g)
1	3.1612	0.5	0.7282
2	3.3831	0.5	0.7191
3	3.3236	0.5	0.7311
4	3.2342	0.5	0.7321
5	3.2126	0.5	0.7224

RESULTS AND DISCUSSION

1. Characterization of XRD Material Fe₃O₄/C18/SiO₂ / [3 (2-Aminoethyl amino) propyl] Trimethoxy silane

Synthesis of Fe₃O₄/C18 was carried out by the sono-coprecipitation method by reacting FeCl₃ with FeSO₄ under alkaline conditions, which was assisted by ultrasonic waves. The result showed a black Fe₃O₄/C18 crystal was suitable with stoichiometric calculations. Furthermore, the coating SiO₂/ [3 (2-aminoethyl amino) propyl] Trimethoxy silane with the results of brown crystals. The success of the coated was shown by increasing the mass of the synthesis results shown in Table 1.

The identification process to determine the success of Fe₃O₄ crystal synthesis was done by looking at the weight of the synthesis results from each treatment. The first synthesis was carried out by comparing data 5 times from the results of Fe₃O₄/C18 synthesis compared with theoretical calculations. For once, the synthesis, according to the result, when it was converted into stoichiometry calculations, was 0.0138 mol. This is the same as the number of moles of FeSO₄·7H₂O salt, which is 0.0138 moles.

According to calculations, there was ± 0.006 mol of Fe lost during the synthesis process. Therefore, the adsorbent was wasted very much. Identification of impurity material arising from the by-products of synthesis was made by comparing the XRD characterization data with JCPDS standard data. Seeing the possibility that occurred during the synthesis process, it needed to do the checking of metal oxides that appeared as a byproduct or further oxidation of Fe

material. The data showed that there was a pollutant in the form of Fe₃O₄, which was shown by JCPDS #.

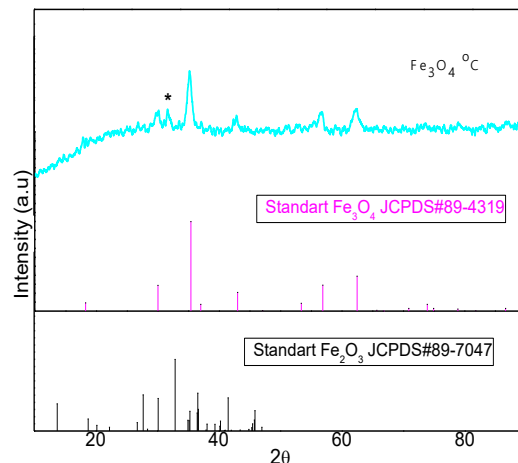


Figure 1. Fe₃O₄/C18 diffraction patterns and impurity identification

One impurity peak was identified as wuestite or Fe₂O₃ at 2θ (31.96) in accordance with JCPDS Fe₂O₃ standard # 89-7047. A comparison of diffraction patterns was also conducted on the XRD results with crystal Fe₃O₄/C18 and Fe₃O₄/C18/ SiO₂/[3(2-aminoethyl amino) propyl] Trimethoxy silane based on Figure 2, it was seen a decline in the intensity of the previous 950.81 into 771.

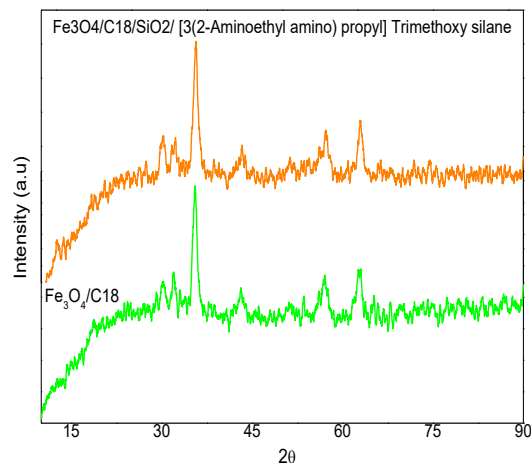


Figure 2. Comparison of diffraction patterns Fe₃O₄/C18 and Fe₃O₄/C18/SiO₂/[3 (2-Aminoethyl amino) propyl] Trimethoxy silane

2. A Functional Testing Groups on material Fe_3O_4 / C18 and $\text{Fe}_3\text{O}_4/\text{C18}/\text{SiO}_2/$ [3(2-Aminoethyl amino) propyl] Trimethoxy silane

Functional group analysis to see the success of coating of SiO_2 material and propyl [3(2-Aminoethyl amino) groups Trimethoxy silane was performed by Fourier Transform Infra-Red characterization, through the appearance of different fingerprint based on each functional group.

The FTIR spectrum was used to determine the modification of the functional group [3(2-Aminoethyl amino) propyl] Trimethoxy silane by looking at the appearance of a fingerprint pattern that resulted from 5 times synthesis. Based on the spectrum showing almost the same pattern, based on the results of the FTIR spectra $\text{Fe}_3\text{O}_4/\text{C18}/\text{SiO}_2/$ [3 (2-Aminoethyl amino) propyl] Trimethoxy silane, It was seen several absorption bands of the synthesis of the Fe_3O_4 core that is in 1527 and is an asymmetric vibration group (COO^-), 1720 shows C=O stretching, while at number 2854 is the symmetry vibration of CH- and 2924 cm^{-1} is the asymmetric vibration of CH_2 originating from the oleic acid group [18].

Synthesis of Fe_3O_4 with the oleic acid protective agent that is bound to the surface of Fe_3O_4 is explained by the formation of the bond between the Fe group COO^- predicted wavelengths in the range of 1720 to 1527 cm^{-1} [19].

Interaction between carboxylate heads and metal atoms was divided into four categories: monodentate, bidentate bridges, bidentate chelating, and ionic interactions. The difference between the asymmetric vibration (COO^-) and the symmetry vibration

(COO^-) is used to strengthen the explanation of the type of interaction between the carboxylic group and the metal atom. If the value of Δ is between ($200\text{-}320\text{ cm}^{-1}$) then it is possible that the interaction that occurs is monodentate interaction, whereas if the price Δ ($<110\text{ cm}^{-1}$) is the result of the interaction of chelating bidentate and in the range ($140\text{-}190\text{ cm}^{-1}$) is bidentate bridge interaction—shown in Figure 3. The price of Δ ($1720\text{-}1527 = 193\text{ cm}^{-1}$) indicates their bidentate bridge interaction between the carboxylate head of the Fe atoms covalently Fe_3O_4 coordination.

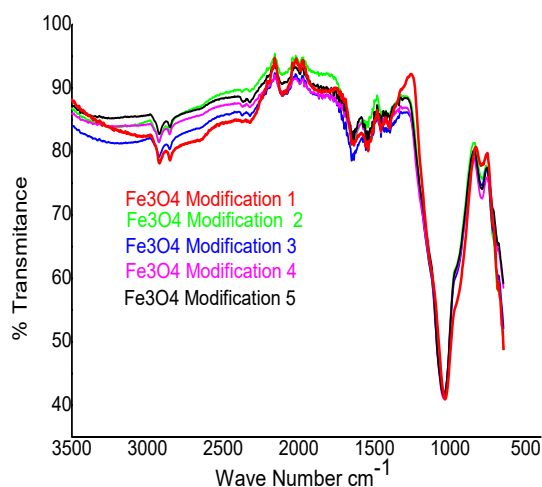


Figure 3. $\text{Fe}_3\text{O}_4/\text{C18}/\text{FTIR}$ Spectra Pattern $\text{SiO}_2/$ [3(2-Aminoethyl amino) propyl] Trimethoxy silane five times the result of the synthesis

The successful synthesis of $\text{Fe}_3\text{O}_4/\text{C18}/\text{SiO}_2/$ [3(2-Aminoethyl amino) propyl] trimethoxy silane crystals is shown by the appearance of a sharp main absorption at 1040 cm^{-1} , which is the Si-O-Si bond that is predicted to cover Fe_3O_4 [20]. Uptake of OH groups originating from silanol and N-H groups is possible to overlap at 3425 cm^{-1} , while the characteristics of NH_2 groups derived from the ethylene function group of

diamino are at wavenumbers 1542 to 1654 cm^{-1} [21].

3. TEM and SEM-EDX $\text{Fe}_3\text{O}_4/\text{C18}/\text{SiO}_2/$ [3(2-Aminoethyl amino) propyl] Trimethoxy silane

Paramagnetic $\text{Fe}_3\text{O}_4/\text{C18}/\text{SiO}_2/$ [3(2-Aminoethyl amino) propyl] Trimethoxy silane was further characterized by using SEM-EDX

to see the shape and size of uniformity of particles and their constituent compositions.

Based on Figure 4, the result of Transmission Electron Microscopy measurements showed long and small crystal beams, which indicated the characteristics of Fe_3O_4 crystals which had.

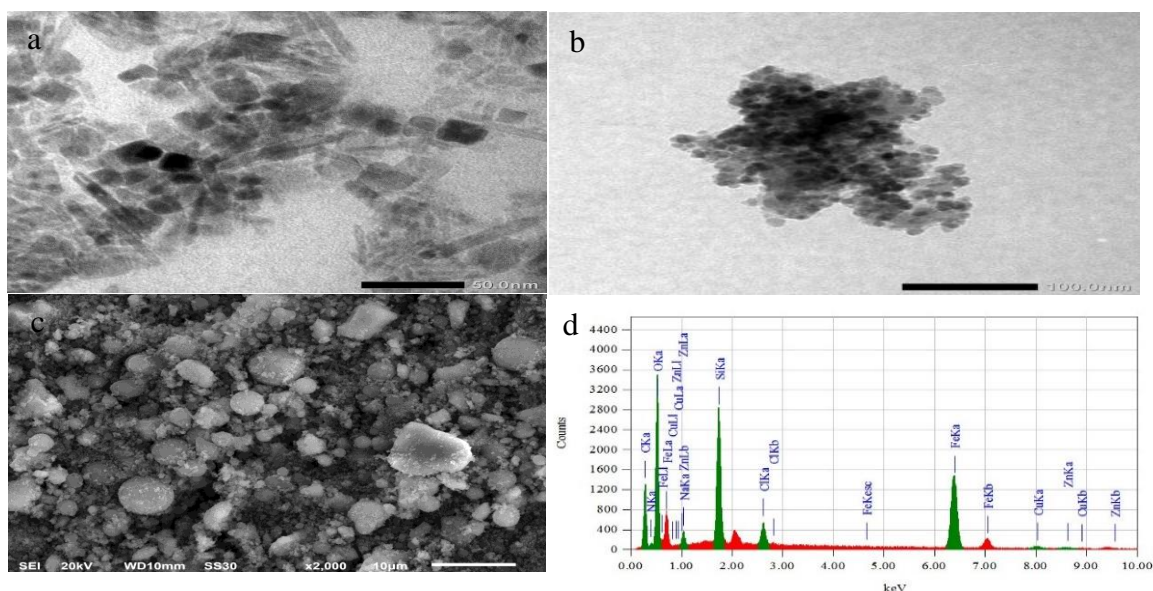


Figure 4. (a) TEM $\text{Fe}_3\text{O}_4 / \text{C18}$ (b) TEM $\text{Fe}_3\text{O}_4/\text{C18}/\text{SiO}_2/$ [3(2-Aminoethyl amino) propyl] Trimethoxy silane, (c) SEM image 2000X and (d) Energy Dispersive-X Ray of Particles $\text{Fe}_3\text{O}_4/\text{C18}/\text{SiO}_2/$ [3(2-Amino ethyl amino) propyl] Trimethoxy silane

Sizes below 50 nm. After coating $\text{SiO}_2/$ [3(2-Aminoethyl amino) propyl] Trimethoxy silane, the size still showed the same thing below 50 nm, but there is a change from cube crystals to spherical or aggregated spheres. This was supported by scanning surface morphology particle using Scanning Electron Microscopy, which showed a fairly uniform size with a small particle size in the form of a sphere, although there were some aggregations forming a large sphere. Based on EDX data, it can be said that the synthesis of $\text{Fe}_3\text{O}_4 / \text{C18} / \text{SiO}_2 /$ [3 (2-Aminoethyl amino) propyl] Trimethoxysilan was successfully

carried out in the presence of 13.49% Fe content, C 25.51%, N 8.58%, O 43, 59% and Si 5.87% which are the largest constituent components of particles[22].

4. Kinetics of adsorption of $\text{Fe}_3\text{O}_4/\text{C18}/\text{SiO}_2/$ [3(2-Aminoethyl amino) propyl] Trimethoxy silane against Cu^{2+} and Cr^{6+} ions

Adsorption kinetics study has been done by studying the adsorption at various pH variations first that were expected to Optimize the adsorption results. Based on Figure 5, it appears that Cu has the best adsorption at pH 7 because at that pH, Cu is in the Cu^{2+} and $\text{Cu}(\text{OH})^+$ species[23].

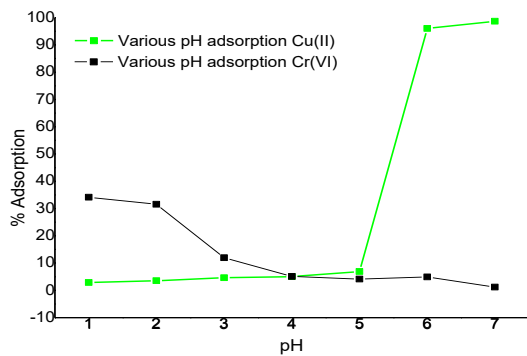


Figure 5. Optimization of pH of adsorption solution Cu^{2+} and Cr^{6+}

The best adsorption of Cr was shown at acidic pH, which indicated that Cr was in a negative species. When the pH is between 0-5 Cr (VI) ion 80% is in the form of HCrO_4^- and the remaining 20% is in the $\text{Cr}_2\text{O}_7^{2-}$ species [24]. NH_3 and NH_2 groups are protonated into NH_3^+ and NH_2^+ so that the Cr ions in the form of HCrO_4^- will interact through electrostatic bonds [25].

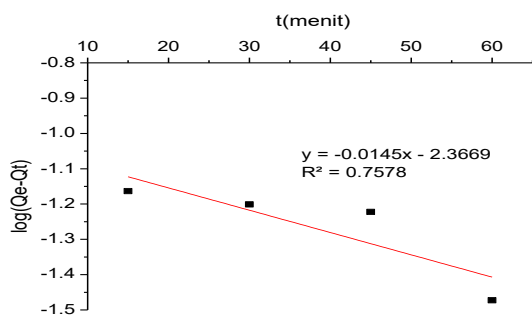


Figure 6. Graph of the kinetics model pseudo first-order adsorption of Cu^{2+}

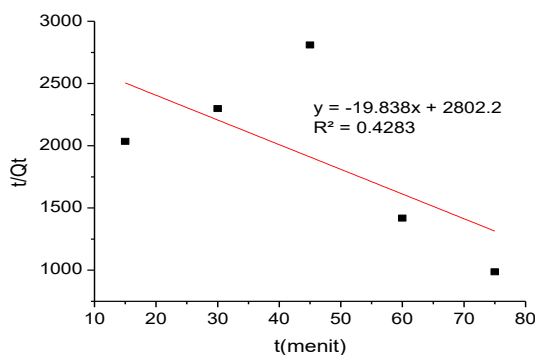


Figure 7. Graph of the kinetics model pseudo second-order adsorption of Cu^{2+}

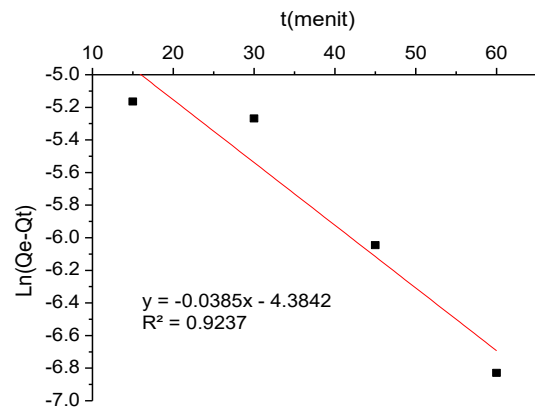


Figure 8. Graph of the kinetics model pseudo first-order adsorption of Cr^{6+}

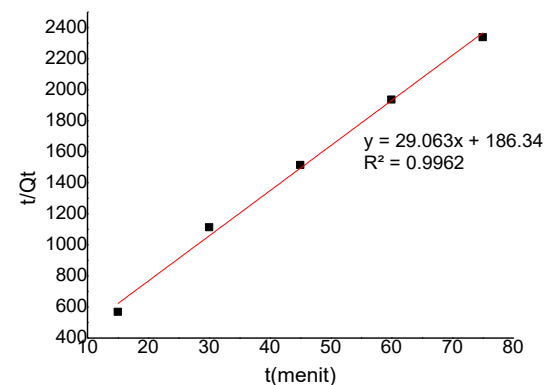


Figure 9. Graph of the kinetics model pseudo Second-order adsorption of Cr^{6+}

The modeling results showed that the Cu adsorption kinetics in the solution system at pH 7 followed the pseudo-order 1 (Lagergreen) model with good linearity. If observed from the adsorption process that occurred H_2O acts as a solvent whose concentration is concentrated, and the concentration of H_2O and H^+ in the solution system was kept constant, because the volume was too large, the contact between the adsorbent particles with the adsorbate will be smaller so that it would affect the course of the adsorption process. This showed that the zero-order adsorption of H_2O and H^+ , so that it can be said that the adsorption runs according to pseudo-1st order (Lagergren).

Table 2. Kinetics Model of the Fe₃O₄/C18/SiO₂/ [3(2-Aminoethyl amino) propyl] Trimethoxy silane) adsorption model for Cu and Cr

Kinetics Model	Adsorption rate (k)	R ²
Pseudo orde-1 Cu	0,0333 min ⁻¹	0,7578
Pseudo orde-2 Cu	0,00105 gmM ⁻¹ min ⁻¹	0,4283
Pseudo orde-1 Cr	0,0887 min ⁻¹	0,954
Pseudo orde-2 Cr	0,00536 gmM ⁻¹ min ⁻¹	0,996

The results of Cr adsorption kinetics modeling showed linear results with the pseudo-order 2 (McKay & Ho) kinetics model with high linearity. The second-order pseudo-adsorption rate constant is a type of chemical adsorption, so it was possible to try to model the adsorption data in the intraparticle diffusion model according to Pseudo-first order. Interparticle diffusion modeling occurred through three stages, the first stage of surface adsorption that occurs very quickly, the second stage of gradual adsorption, and the third is the equilibrium adsorption that occurs very slowly [26].

CONCLUSION

Synthesis of Fe₃O₄/C18/SiO₂/[3(2-Aminoethyl amino) propyl] Trimethoxy silane has been successfully carried out. Coating of the amine group which is a source of electron donors. The success of the synthesis of Fe₃O₄/C18 cores can be clarified by XRD characterization. While SiO₂ and the [3(2-Amino ethyl amino) propyl] grouping Trimethoxy silane were shown through FTIR analysis with the appearance of the fingerprint band characteristic of the NH₂ group derived from the ethylene function group of diamino at the wavenumber

1542cm⁻¹. The size of the synthesis material indicates the size of the nano. The composition of the material also shows the presence of elements C, N, O, and Si. For the kinetics of adsorption of material against Cu according to the pseudo order one kinetics model with an adsorption rate of 0.0333 min⁻¹, while for Cr in accordance with pseudo-order-2 with an adsorption rate of 0.00536 gmM⁻¹min⁻¹.

ACKNOWLEDGMENTS

Acknowledgments the author was given to the Directorate General of Higher Education for grants No. 112/SP2H/LT/DPRM/2019 and related ones who assisted in the completion of this study.

REFERENCES

- [1] L. Zhang, R. He, & H. C. Gu, "Oleic acid coating on the monodisperse magnetite nanoparticles," *Appl. Surf. Sci.*, vol. 253, no.5, pp. 2611-2617, 2006.
[DOI:10.1016/j.apsusc.2006.05.023](https://doi.org/10.1016/j.apsusc.2006.05.023)
- [2] M. Faraji, Y. Yamini, & M. Rezaee, "Magnetic nanoparticles: Synthesis, stabilization, functionalization, characterization, and applications," *Journal of the Iranian Chemical Society*, vol. 7, no.1, pp. 1-37, 2010.
[DOI:10.1007/BF03245856](https://doi.org/10.1007/BF03245856)
- [3] W. W. Yu, J. C. Falkner, C. T. Yavuz, & V. L. Colvin, "Synthesis of monodisperse iron oxide nanocrystals by thermal decomposition of iron carboxylate salts," *Chem. Commun.*, vol. 20, pp. 2306-2307, 2004.
[DOI:10.1039/B409601K](https://doi.org/10.1039/B409601K)
- [4] Y. Wang, I. Nkurikiyimfura, & Z. Pan, "Sonochemical Synthesis of Magnetic Nanoparticles," *Chem. Eng. Commun.*, vol. 202, no. 5, pp. 616-621, 2015.
[DOI:10.1080/00986445.2013.858039](https://doi.org/10.1080/00986445.2013.858039)

- [5] V. A. J. Silva, P. L. Andrade, M. P. C. Silva, A. D. Bustamante, L. De Los Santos Valladares, & J. Albino Aguiar, "Synthesis and characterization of Fe₃O₄ nanoparticles coated with fucan polysaccharides," *J. Magn. Mater.*, vol. 343, pp. 138-143, 2013.
DOI:10.1016/j.jmmm.2013.04.062
- [6] E. S. Jang, "Preparation of Fe₃O₄/SiO₂ core/shell nanoparticles with ultrathin silica layer," *J. Korean Chem. Soc.*, vol. 56, no. 4, pp. 478-483, 2012.
DOI:10.5012/jkcs.2012.56.4.478
- [7] N. Mahmed, Development of Multifunctional Magnetic Core Nanoparticles. Espoo: School of Chemical Technology, 2013.
Google Scholar
- [8] Y. H. Deng, C. C. Wang, J. H. Hu, W. L. Yang, & S. K. Fu, "Investigation of formation of silica-coated magnetite nanoparticles via sol-gel approach," *Colloids Surfaces A Physicochem. Eng. Asp.*, vol. 262, no. 1-3, pp. 87-93, 2005.
DOI:10.1016/j.colsurfa.2005.04.009
- [9] M. E. Khosroshahi & L. Ghazanfari, "Preparation and characterization of silica-coated iron-oxide nanoparticles under N₂ gas," *Phys. E Low-Dimensional Syst. Nanostructures*, vol. 2, no. 6, pp. 1824-1829, 2010.
DOI:10.1016/j.physe.2010.01.042
- [10] W. Wu, Q. He, & C. Jiang, "Magnetic iron oxide nanoparticles: Synthesis and surface functionalization strategies," *Nanoscale Res. Lett.*, vol. 3, no. 11, pp. 397, 2008.
DOI:10.1007/s11671-008-9174-9
- [11] P. Ashtari, X. He, K. Wang, & P. Gong, "An efficient method for recovery of target ssDNA based on amino-modified silica-coated magnetic nanoparticles," *Talanta*, vol. 67, no. 3, pp. 548-554, 2005.
DOI:10.1016/j.talanta.2005.06.043
- [12] Z. Zhang, H. Li, J. Li, X. Li, Z. Wang, X. Liu, & L. Zhang, "A novel adsorbent of core-shell construction of chitosan-cellulose magnetic carbon foam: Synthesis, characterization and application to remove copper in wastewater," *Chem. Phys. Lett.*, vo.731,2019.
DOI:10.1016/j.cplett.2019.07.001
- [13] M. Mirzaeinejad, Y. Mansoori, & M. Amiri, "Amino functionalized ATRP-prepared polyacrylamide-g-magnetite nanoparticles for the effective removal of Cu(II) ions: Kinetics investigations," *Mater. Chem. Phys.*, vol. 205, pp. 195-205, 2018.
DOI:10.1016/j.matchemphys.2017.11.020
- [14] D. Zhao, X. Gao, C. Wu, R. Xie, S. Feng, & C. Chen, "Facile preparation of amino functionalized graphene oxide decorated with Fe₃O₄ nanoparticles for the adsorption of Cr(VI)," *Appl. Surf. Sci.*, vol. 384, pp.1-9, 2016.
DOI:10.1016/j.apsusc.2016.05.022
- [15] J. Li, X. Miao, Y. Hao, J. Zhao, X. Sun, & L. Wang, "Synthesis, amino-functionalization of mesoporous silica and its adsorption of Cr(VI)," *J. Colloid Interface Sci.*, vol. 318, no. 2, pp. 309-314, 2008.
DOI:10.1016/j.jcis.2007.09.093
- [16] T. Shahwan, "Lagergren equation: Can maximum loading of sorption replace equilibrium loading?," *Chem. Eng. Res. Des.*, vol. 96, pp. 172-176, 2015.
DOI:10.1016/j.cherd.2015.03.001
- [17] Y. S. Ho and G. McKay, "Pseudo-second order model for sorption processes," *Process Biochem.*, vol. 34, no. 5, pp. 451-465, 1999.
DOI:10.1016/S0032-9592(98)00112-5
- [18] G. V. M. Jacintho, A. G. Brolo, P. Corio, P. A. Z. Suarez, & J. C. Rubim, "Monodisperse MFe₂O₄ (M = Fe, Co, Mn) Nanoparticles," *J. Phys. Chem. C*, vol. 126, no. 1, pp. 273-279, 2009.
DOI:10.1021/ja0380852
- [19] J. Liang, H. Li, J. Yan, & W. Hou, "Demulsification of oleic-acid-coated magnetite nanoparticles for cyclohexane-in-water nanoemulsions," *Energy and Fuels*, vol. 28, no. 9, pp. 6172-6178, 2014.
DOI:10.1021/ef501169m

- [20] A. R. Keshtkar, M. Irani, & M. A. Moosavian, "Removal of uranium (VI) from aqueous solutions by adsorption using a novel electrospun PVA/TEOS/APTES hybrid nanofiber membrane: Comparison with casting PVA/TEOS/APTES hybrid membrane," *J. Radioanal. Nucl. Chem.*, vol. 295, no. 1, pp. 563-571, 2013.
[DOI:10.1007/s10967-012-2110-6](https://doi.org/10.1007/s10967-012-2110-6)
- [21] Y. Takeda, Y. Komori, & H. Yoshitake, "Direct stöber synthesis of mono-disperse silica particles functionalized with mercapto-, vinyl- and amino-propylsilanes in alcohol-water mixed solvents," *Colloids Surfaces A Physicochem. Eng. Asp.*, vol. 422, pp. 68-74, 2013.
[DOI:10.1016/j.colsurfa.2013.01.024](https://doi.org/10.1016/j.colsurfa.2013.01.024)
- [22] Y. Zhang, Q. Xu, S. Zhang, J. Liu, J. Zhou, H. Xu, H. Xiao, & J. Li, "Preparation of thiol-modified Fe₃O₄.2SiO₂ nanoparticles and their application for gold recovery from dilute solution," *Sep. Purif. Technol.*, vol. 116, pp. 391-397, 2013.
[DOI:10.1016/j.seppur.2013.06.018](https://doi.org/10.1016/j.seppur.2013.06.018)
- [23] K. J. Powell, P. L. Brown, R. H. Byrne, T. Gajda, G. Hefter, S. Sjöberg, & H. Wanner, "Chemical speciation of environmentally significant metals with inorganic ligands. PART 2: The Cu²⁺-OH-, Cl-, CO₃²⁻, SO₄²⁻, and PO₄³⁻ systems (IUPAC Technical Report)," in *Pure and Applied Chemistry*, vol. 79, no. 5, pp. 895-950, 2007.
[DOI:10.1016/j.seppur.2013.06.018](https://doi.org/10.1016/j.seppur.2013.06.018)
- [24] G. P. Gallios & M. Vaclavikova, "Removal of chromium (VI) from water streams: A thermodynamic study," *Environ. Chem. Lett.*, vol.6, no.4, pp. 235-240, 2008.
[DOI:10.1007/s10311-007-0128-8](https://doi.org/10.1007/s10311-007-0128-8)
- [25] N. Mao, L. Yang, G. Zhao, X. Li, & Y. Li, "Adsorption performance and mechanism of Cr(VI) using magnetic PS-EDTA resin from micro-polluted waters," *Chem. Eng. J.*, vol. 200, pp. 480-490, 2012.
[DOI:10.1016/j.cej.2012.06.082](https://doi.org/10.1016/j.cej.2012.06.082)
- [26] H. Li, D. L. Xiao, H. He, R. Lin, and P. L. Zuo, "Adsorption behavior and adsorption mechanism of Cu(II) ions on amino-functionalized magnetic nanoparticles," *Trans. Nonferrous Met. Soc. China (English Ed.)*, vol.23, no.9, pp. 2657-2665, 2013.
[DOI:10.1016/S1003-6326\(13\)62782-X](https://doi.org/10.1016/S1003-6326(13)62782-X)